Journal of Applied Polymer Science

Preparation, physical, and mechanical properties of soy protein isolate/guar gum composite films prepared by solution casting

Chunxia Sui,[1] Wenzhao Zhang,[1] Fei Ye,[1] Xiaoming Liu,[2] Guoping Yu[3]

[1]College of Science, Northeast Agricultural University, Harbin Heilongjiang 150030, China

[2]Department of Mechanical Engineering, Heilongjiang Agricultural Engineering Vocational College, Harbin Heilongjiang 150088, China

[3]College of Food, Northeast Agricultural University, Harbin Heilongjiang 150030, China

Correspondence to: F. Ye (E-mail: yefei@neau.edu.cn)

ABSTRACT: Guar gum (GG) was incorporated into soy protein isolate (SPI) films using a blending solution casting method to form SPI/GG composite films. The effects of SPI and GG contents on the transparency, water susceptibility, mechanical, and gas-barrier properties of SPI/GG composite films were analyzed. The results showed that SPI/GG composite films with added GG were much more tensile-resistant, water-resistant, gas-barrier properties but less deformable property than SPI control film. The presence of GG also improved film barrier to the light. The analysis results of contact angle measurement, Fourier transform infrared spectroscopy, and scanning electron microscope indicated that GG induced increased network compactness of the composite films which resulted from strong intermolecular interactions, such as hydrogen bonding, that existed between SPI and GG. Findings indicate that GG may be used as a natural means to improve specific properties of SPI films. © 2016 Wiley Periodicals, Inc. J. Appl. Polym. Sci. **2016**, *133*, 43382.

KEYWORDS: composites; films; mechanical properties; properties and characterization; proteins

Received 19 June 2015; accepted 22 December 2015

DOI: 10.1002/app.43382

INTRODUCTION

With enhancing awareness of environmental protection and energy conservation, researchers are increasingly committed to developing biological polymer films for application in the food packing and coating industries.[1,2] These films are mainly derived from natural polymers, including protein, starch, cellulose, and chitosan.[3–8] Not only does protein offer greater film forming properties than polysaccharide, but the film's mechanical and gas-barrier properties are also superior.[9,10] Owing to the abundance, reproducibility, safety, nontoxicity and biodegradability, protein has become an irreplaceable choice in the edible packing or coating field.[11–13] Compared with plastic products synthesized from petroleum, the mechanical and water-resistant properties of protein materials are inferior, which dramatically constrains the potential applications of protein films.[11]

Soy protein (SP), extracted from bean pulps, an produce soy protein concentrate (SPC) and soy protein isolate (SPI) via purification and separation methods, with SPI possessing better film forming ability.[14] 90% of SP is storage protein, mainly consisting of 7S (β-conglycinin) and 11S (glycinin).[15,16] Globin is formed via hydrogen bonds and hydrophobic interactions between the protein subunits. Under alkaline conditions, globin dissociation causes protein chain expanding and interaction with additive components in the system, which facilitates the expansion of the protein's application for food packaging or coating field.[17]

Guar gum (GG) is a natural water-soluble polysaccharide extracted from Indian cluster beans, and is a galactomannan straight chain with the galactose side chains, which determines the characteristics of GG.[18] For instance, Garti *et al.* found that GG had wonderful surface, interfacial, and emulsifiable activities.[19] Cui *et al.* found that complexes could be formed through GG interacting with other linear polysaccharides (e.g., xanthan gum, agarose, and starch).[20] Under the controlled pH reaction conditions, GG molecules can chemically crosslink with crosslinking agents to form films with varying integrities.[21] Therefore, GG and its derivatives are currently extensively applied in food, medicine, and papermaking fields.[22]

Presently, there are many published studies on the preparation and properties improvement of SP films through physical, chemical, and enzymatic modifications.[23] However, SP film's water sensitivity problem and its mechanical properties are always the key points of the research.[24] Due to the complementary advantages conferred by natural polymers, blending two or several natural polymers is an effective way to improve film properties.[5,6,11,16,21]

Table I. Water Uptake of SPI Control Films and SPI/GG Composite Films

SPI:GG		WU (%)
	IG3	
3.0 g:0.00 g	IG3-0	30.6 ± 3.6^{a}
3.0 g:0.15 g	IG3-3	25.2 ± 4.2^{bc}
3.0 g:0.20 g	IG3-4	16.6 ± 1.2^{e}
3.0 g:0.25 g	IG3-5	7.8 ± 1.3^{f}
	IG4	
4.0 g:0.00 g	IG4-0	29.8 ± 5.2^{a}
4.0 g:0.15 g	IG4-3	21.3 ± 0.2^{cd}
4.0 g:0.20 g	IG4-4	21.7 ± 0.4^{cd}
4.0 g:0.25 g	IG4-5	19.4 ± 0.3^{cde}
	IG5	
5.0 g:0.00 g	IG5-0	28.6 ± 1.6^{ab}
5.0 g:0.15 g	IG5-3	22.1 ± 0.2^{cd}
5.0 g:0.20 g	IG5-4	22.7 ± 0.4^{cd}
5.0 g:0.25 g	IG5-5	20.4 ± 0.6^{cde}

All values were average ± SD of three values. Reported average values for all parameters within a column with same superscripts (a, b, c, d, e, and f) are not significantly different ($P < 0.05$).

Thus, in this article, SPI/GG composite films were prepared in the method of a blending solution casting so as to obtain superior properties. Meanwhile, the influences of SPI and GG concentration on the films' transparency, water susceptibility, mechanical, and gas-barrier properties were investigated. In addition, Fourier transform infrared spectroscopy (FTIR), scanning electron microscope (SEM) analyses were performed to analyze the films' structure and morphology characteristics. Finally, water static dripping contact angle measurements were taken to assess film surface hydrophobicity.

MATERIALS AND METHODS

Materials

SPI was purchased from Harbin Hi-tech Soybean Food. Measurement results of SPI by the Kjeldahl determination are: water 5.31%, protein 91.60%, and ash 4.51%. GG, imported from India, was purchased from Tianjin Huayu Economic and Trade. Theremaining reagents used were domestic analytical reagents.

Preparation of Control Films and SPI/GG Composite Films

Using glycerol as the plasticizer, SPI films were prepared using a blending solution casting method. More specifically, different concentrations of SPI powder (3.0, 4.0, 5.0, and 6.0% (w/v)) were evenly dispersed in 100 mL deionized water and absolute ethyl alcohol (4:1 (v/v)). Glycerol (1.5 g) was then added. The solution (pH 7.0 ± 0.1) was first stirred at 30 ± 1 °C to a homogeneous state, heated at 80 ± 1 °C for 30 min, and then cooled at room temperature. After 5 min of ultrasonic defoaming, the solution was cast into a 20 × 20 cm^2 self-made glass mold. The films were peeled off after natural drying. According to the SPI amount, the films were marked with IG3-0, IG4-0, IG5-0, and IG6-0 (as shown in Tables (I–IV)), which were employed as the control films containing no GG.[25]

The SPI solution was prepared in the similar way which was used for preparing control film solution. Then, the GG (0.15, 0.20, and 0.25 g) was added to each SPI solution so as to prepare the SPI/GG composite films. The composite films were formed in the same way which was used for control films and marked as shown in Table III. The IG3 series refers to 3% (w/v) SPI concentration, GG concentrations are 0.00, 0.15, 0.20, 0.25% (w/v), corresponding to control film IG3-0 and SPI/GG composite films IG3-3, IG3-4, and IG3-5, respectively. IG4, IG5, and IG6 are analogous. Before measurement, all film specimens were placed in a 25 °C, 90% relative humidity sealed chamber for 48 h balance.

Physical Properties

A manual spiral micrometer caliper (0.001 mm) was used to measure film thickness (FT) for the measurement of water vapor, O_2, and CO_2 permeability (WVP, OP, and COP), transparency, and tensile properties, respectively, at five random points and the average value was obtained by reference to Han *et al.*[8]

The films were cut into 1 × 4.5 cm^2 strips, which were attached to one side of a cuvette. The transparency was determined as the light transmittance (T, %) in the spectrum (310, 350, 400, 500, 600, and 700 nm) of each sample, which was measured using a 722-spectrophotometer (Shanghai Precision Scientific Instrument) in accordance with ASTM D1746. The T of an empty cuvette was used as the control.

The moisture content was gravimetrically determined (ASTM D644-94, 1994). Three specimens of each film were weighed (m_w) and subsequently dried in an air-circulating oven at 105 °C for 24 h. After this time, films were reweighed (m_0). The moisture content (MC, %) of the sample was calculated as[16]:

$$\mathrm{MC}(\%) = \frac{m_w - m_0}{m_w} \times 100 \quad (1)$$

Table II. Moisture Content of SPI Control Films and SPI/GG Composite Films

SPI:GG		MC (%)
3.0 g:0.00 g	IG3-0	20.7 ± 6.4^{ac}
4.0 g:0.00 g	IG4-0	18.2 ± 1.4^{cd}
5.0 g:0.00 g	IG5-0	18.6 ± 0.5^{cd}
3.0 g:0.15 g	IG3-3	24.6 ± 1.0^{ab}
4.0 g:0.15 g	IG4-3	21.6 ± 0.2^{abc}
5.0 g:0.15 g	IG5-3	18.5 ± 1.1^{cd}
3.0 g:0.20 g	IG3-4	25.4 ± 1.9^{b}
4.0 g:0.20 g	IG4-4	21.0 ± 0.6^{ac}
5.0 g:0.20 g	IG5-4	16.0 ± 0.3^{d}
3.0 g:0.25 g	IG3-5	21.8 ± 3.2^{abc}
4.0 g:0.25 g	IG4-5	20.9 ± 0.8^{ac}
5.0 g:0.25 g	IG5-5	15.4 ± 1.3^{d}

All values were average ± SD of three values. Reported average values for all parameters within a column with same superscripts (a, b, c, and d) are not significantly different ($P < 0.05$).

Table III. Tensile Strength, Breaking Elongation, and Tensile Modulus of SPI Control Films and SPI/GG Composite Films

SPI:GG		TS (MPa)	BE (%)	TM (MPa)
	IG3			
3.0 g:0.00 g	IG3-0	3.62 ± 0.08^{a}	71.0 ± 8.4^{f}	3.0 ± 2.5^{a}
3.0 g:0.15 g	IG3-3	3.58 ± 0.07^{a}	66.6 ± 10.8^{ef}	3.2 ± 1.1^{a}
3.0 g:0.20 g	IG3-4	3.87 ± 0.04^{ab}	65.3 ± 2.4^{ef}	4.8 ± 1.3^{a}
3.0 g:0.25 g	IG3-5	4.44 ± 0.07^{bc}	57.8 ± 4.9^{e}	7.6 ± 1.4^{a}
	IG4			
4.0 g:0.00 g	IG4-0	4.04 ± 0.04^{ab}	55.0 ± 2.7^{de}	23.1 ± 4.8^{a}
4.0 g:0.15 g	IG4-3	4.19 ± 0.13^{ab}	44.9 ± 5.9^{cd}	27.4 ± 9.9^{ab}
4.0 g:0.20 g	IG4-4	4.46 ± 0.18^{bc}	40.5 ± 4.5^{bc}	55.9 ± 14.1^{bc}
4.0 g:0.25 g	IG4-5	5.05 ± 0.16^{c}	37.7 ± 1.3^{bc}	60.5 ± 14.1^{cd}
	IG5			
5.0 g:0.00 g	IG5-0	8.58 ± 0.35^{e}	30.6 ± 2.2^{ab}	70.9 ± 7.4^{cde}
5.0 g:0.15 g	IG5-3	8.41 ± 0.15^{e}	28.7 ± 2.0^{ab}	77.6 ± 15.2^{cde}
5.0 g:0.20 g	IG5-4	13.20 ± 0.08^{g}	19.4 ± 1.6^{a}	78.1 ± 3.6^{cde}
5.0 g:0.25 g	IG5-5	14.92 ± 0.10^{h}	19.7 ± 0.6^{a}	90.2 ± 6.4^{de}
	IG6			
6.0 g:0.00 g	IG6-0	10.64 ± 0.50^{f}	60.4 ± 5.2^{ef}	163.7 ± 32.9^{f}
6.0 g:0.15 g	IG6-3	6.98 ± 0.23^{d}	56.7 ± 4.2^{e}	146.7 ± 5.4^{f}
6.0 g:0.20 g	IG6-4	7.54 ± 0.09^{d}	30.8 ± 2.6^{ab}	90.9 ± 14.5^{de}
6.0 g:0.25 g	IG6-5	8.00 ± 0.23^{de}	60.4 ± 3.7^{ef}	99.9 ± 27.9^{e}

The different letters (a, b, c, d, e, f, and g) indicate significant differences between data in the same column ($P < 0.05$, $n = 3$).

Table IV. H_2O, O_2, and CO_2 Permeability of SPI Control Films and SPI/GG Composite Films

SPI:GG		WVP* ($mg \cdot mm \cdot h^{-1} \cdot m^{-2} \cdot kPa^{-1}$)	OP#* ($g \cdot day^{-1} \cdot m^{-2}$)	COP##* ($g \cdot day^{-1} \cdot m^{-2}$)
	IG3			
3.0 g:0.00 g	IG3-0	79 ± 9^{a}	2.44 ± 0.09^{c}	16.1 ± 0.5^{f}
3.0 g:0.15 g	IG3-3	105 ± 5^{bc}	2.33 ± 0.11^{c}	15.2 ± 0.1^{f}
3.0 g:0.20 g	IG3-4	126 ± 5^{cd}	2.15 ± 0.07^{c}	15.2 ± 0.1^{f}
3.0 g:0.25 g	IG3-5	87 ± 3^{ab}	1.72 ± 0.07^{b}	9.5 ± 0.4^{de}
	IG4			
4.0 g:0.00 g	IG4-0	105 ± 7^{bc}	2.15 ± 0.20^{c}	10.7 ± 0.3^{e}
4.0 g:0.15 g	IG4-3	149 ± 9^{ef}	1.76 ± 0.07^{b}	8.3 ± 0.5^{cd}
4.0 g:0.20 g	IG4-4	173 ± 7^{g}	1.76 ± 0.07^{b}	7.9 ± 0.4^{bcd}
4.0 g:0.25 g	IG4-5	114 ± 6^{c}	1.61 ± 0.05^{b}	9.1 ± 0.3^{cde}
	IG5			
5.0 g:0.00 g	IG5-0	137 ± 4^{de}	0.78 ± 0.13^{a}	9.2 ± 1.2^{cde}
5.0 g:0.15 g	IG5-3	162 ± 7^{fg}	0.72 ± 0.20^{a}	7.4 ± 1.2^{abc}
5.0 g:0.20 g	IG5-4	201 ± 9^{h}	0.65 ± 0.00^{a}	6.4 ± 0.1^{ab}
5.0 g:0.25 g	IG5-5	177 ± 5^{g}	0.65 ± 0.13^{a}	6.0 ± 0.5^{a}
Synthetic films HDPE**		13.5 ± 1.0	60.1 ± 12.4	117.4 ± 11.3

The different superscripts (a, b, c, d, e, f, and g) indicate significant differences between data in the same column ($P < 0.05$, $n = 3$).
#The O_2 pressure difference between the film internal and external side is 21.2 kPa.
##The CO_2 pressure difference between the film internal and external side is 30.4 Pa.
*The average thickness for H_2O, O_2, and CO_2 permeability was 0.103 ± 0.02 mm.
**HDPE (high-density polyethylene films),[38] units for permeability are $cm^3 \cdot \mu m \cdot m^{-2} \cdot day^{-1} \cdot kPa^{-1}$.

The water uptake was determined used 10 × 10 mm^2 samples of films at room temperature following a reported method. After weighing to determine the initial weight (m_0), they were placed in a container conditioned at 98% RH using a saturated copper sulfate solution. At specific time intervals, the sample weight (m_t) was determined until an equilibrium value was reached. Three replicates were tested for each sample. The water uptake (WU, %) of the sample was calculated as[26,27]:

$$WU(\%)=\frac{m_t-m_0}{m_0}\times 100 \quad (2)$$

Film wettability was measured through the contact angle with a contact angle meter (Digidrop, GBX, France). Distilled water was dripped onto sample films attached to horizontal metal sheets using 10-μm-diameter needle tubing. A DH-HV1303UM digital video camera was used to measure the contact angle (θ). The average of five measurements was taken as the result.

Mechanical Properties

The films were cut into I-shaped strips. ATA.XT.Plus Texture Analyzer (British Stable Micro System Company) was employed to measure mechanical strength by the following standard ASTM D882 method at a tension speed of 5 mm/s. The effective tension distance was 100 mm. The tensile strength (TS, MPa) at film breaking and the film length (L_1, cm) from tension to breaking were recorded. The initial film length was expressed as L_0 (cm). Three samples were measured for each film and the average value was obtained. Tensile modulus (TM, MPa) was determined as the slope of the linear regression performed on the first points (~10) of the stressstrain curves. The breaking elongation (BE, %) was derived from the following equation[28]:

$$BE(\%)=\frac{L_1-L_0}{L_0}\times 100 \quad (3)$$

Permeability Properties

Water vapor permeability (WVP) was measured using the modified standard test method (ASTM Standard E96M-10, 2010). Anhydrous calcium chloride was ground down to particles 2 mm in diameter before incubation at 200 °C for 2 h. After cooling, the particles were transferred to a 50-mL conical flask to 0.5 cm under the bottleneck. The uniform, unmarked, and imperforate films were measured for FT, wax-sealed at the bottleneck, and weighted. Then, the conical flask was placed in a 25 ± 1 °C, sealed chamber (100% RH), and predrenched for 12 h so as to obtain a constant vapor pressure difference between the films' internal and external side (the vapor pressure of 25 °C pure water calculated as 3.1671 kPa). The flask was then weighed after stabilization and weight measurements were taken after 24 h. Δm was the mean value of 5 measurements. WVP was derived according to the following equation[29]:

$$WVP=\frac{\Delta m\times d}{A\times t\times \Delta p} \quad (4)$$

where WVP is the water vapor permeability ($mg\cdot mm\cdot h^{-1}\cdot m^{-2}\cdot kPa^{-1}$); Δm is the water vapor migration amount; A is the drenching area (m^2); t is the drenching stabilization time interval (h); d is the FT (mm); and Δp is the water vapor pressure difference between the film internal and external side (kPa).

In accordance with modified standard test method (ASTM standard method D3985), 2 mL of linoleic acid was added to a 50-mL conical flask, the bottleneck of which was wax-sealed with SPI film. At room temperature, the samples' weight was measured once per day for 1 week. The O_2 permeability (OP, $g\cdot day^{-1}\cdot m^{-2}$) was calculated based on the increased mass of the conical flask (Δm, g), permeation area (A, m^2) and time interval (t, days). For each sample, the measurement was repeated three times and the average value was obtained. The O_2 permeability equation is as follows[30]:

$$OP=\frac{\Delta m}{A\times t} \quad (5)$$

About 5-mL saturated KOH solution was added into the 50-mL conical flask, the bottleneck of which was wax-sealed with SPI film. The measurement is the same as in section 2.7. CO_2 permeability (COP, $g\cdot day^{-1}\cdot m^{-2}$) could be derived from the following equation[30]:

$$COP=\frac{\Delta m}{A\times t} \quad (6)$$

Morphological and Structure Properties

To evaluate the interaction of SPI and GG components of the composite films, a Nicolet/Nexus 670 infrared spectrometric analyzer was employed to analyze the structure of the control and SPI/GG composite films. The sample films were dried at 50 °C, grounded into powder, and then mixed with KBr during the determination of FTIR. The scanning scope ranged from 400 to 4000 cm^{-1}.

S-3400N SEM (Hitachi, Japan) was adopted to observe the films' surface and sectional microtopography. Sample films were dried at 50 ± 1 °C and cut into 1 × 5 mm^2 small pieces by a razor blade before test, were vertically or horizontally fixed on the sample stage, gold plated under vacuum for 20 min, and then taken out for analysis.

Statistical Analysis

The statistical data was analyzed using SPSS 18.0 (SPSS, 160 Chicago). All data were presented as the mean values ± standard deviation. Differences were considered at a significant level of 95% ($P<0.05$).

RESULTS AND DISCUSSION

Appearance

SPI/GG composite films prepared by casting with different concentrations of SPI and GG were homogeneous, translucent, and slightly brownish, with a general visual appearance similar to the control SPI films.

Film Thickness

All film samples had thicknesses in the range of 0.101 − 0.105 mm. Film thickness was found to be unaffected ($P>0.05$) by the examining concentration range of SPI and GG. Therefore, the difference, if any, in the film properties should not be the result of FT.

Transparency (*T*, %)

Variations in *T* of SPI control films [G3-0, IG4-0, IG5-0, and IG6-0, Figure 1(a)] and SPI, SPI/GG composite films [IG3-0, IG3-3, IG3-4, and IG3-5, Figure 1(b)] were observed with varying SPI and GG concentrations under 310, 350, 400, 500, 600, and 700 nm in the ultraviolet visible light wavelength ranges. Transparency may be affected by various factors including FT.[31] In this study, however, there was insignificant difference in average thickness among prepared films. The transparency of films in the low wavelength, especially ultraviolet ranges, was significantly lower than that of visible light. The experiment found that the transparency of SPI/GG composite films was close to zero when the wavelength of incident light was under 300 nm.[16] Meanwhile, the transparency of the films decreased with increasing SPI concentration within the low wavelength ranges. This is consistent results from Li *et al.*, where SPI films displayed UV light-barrier properties[32] and may be related to the amount of aromatic amino groups in SPI molecules.[16] When the wavelength of incident light was above 500 nm, the transparency of the SPI control films maintained relatively stable, between 80 and 90% for the various SPI concentrations. For the SPI/GG composite film, the transparency decreased with increasing GG concentrations for all wavelengths measured (as found for all series, 4, 5, and 6). This indicates that GG contributes to reducing SPI film' transparency, which provides a solid foundation for the future application of SPI/GG composite films in food packing.

Water Susceptibility

Tables I and II report the MC and WU for films with different SPI and GG concentrations. We observed a slight decrease in the property studied as WU with the increasing of GG proportion at the same SPI concentration from Table I. The property studied as MC showed a slight decrease with the increasing of SPI proportion at the same GG concentration as shown in Table II. Considering that both components, GG and protein matrix are hydrophilic, it is evident that in these films the interactions between the components, possibly through the formation of hydrogen bridges, would leave fewer sites available to absorb water.[26] The decrease in WU and MC with the addition of GG could also be due to an increase in film surface hydrophobicity, as was evidenced by increasing contact angle for IG5-0, IG5-3, and IG5-4 films (Figure 2). This can be attributed to SPI/GG interactions, leaving a lower concentration of hydrophilic groups exposed towards film surface.

Water static dripping contact angle measurements offer a viable approach to characterize film surface hydrophobicity, where a larger contact angle is indicative of greater surface hydrophobicity.[33] In order to study the effect of GG addition on surface hydrophobicity of SPI films, the water drop dispersion conditions and the corresponding contact angles were investigated for IG5-0, IG5-3, IG5-4, and IG5-5 (Figure 2), as they displayed the best mechanical properties and permeability. The composite films showed a decrease in surface hydrophobicity with increasing GG concentrations. However, an exception to this trend can be found for addition of GG at lower concentration of 0.2% (w/v), causing a relative increase in surface hydrophobicity. This may be caused by interactions between the abundance of hydrophilic amino acids in SPI molecules and polyhydroxy in GG molecules. Nonetheless, the surface hydrophobicity of composite films did not show a uniform decrease in hydrophobicity across the series, suggesting that the GG/SPI interactions vary at different GG concentrations. Specifically, SPI and GG mainly interact with hydrogen bonds at GG concentrations between 0.15 and 0.20% (w/v) so that the ratio of hydrophobic to hydrophilic residues is increased, increasing the overall hydrophobicity[16]; while at GG concentrations of 0.20 and 0.25% (w/v), the compatibility between SPI and GG change, causing decreased surface hydrophobicity, which is in agreement with SEM analysis (Figure 4).

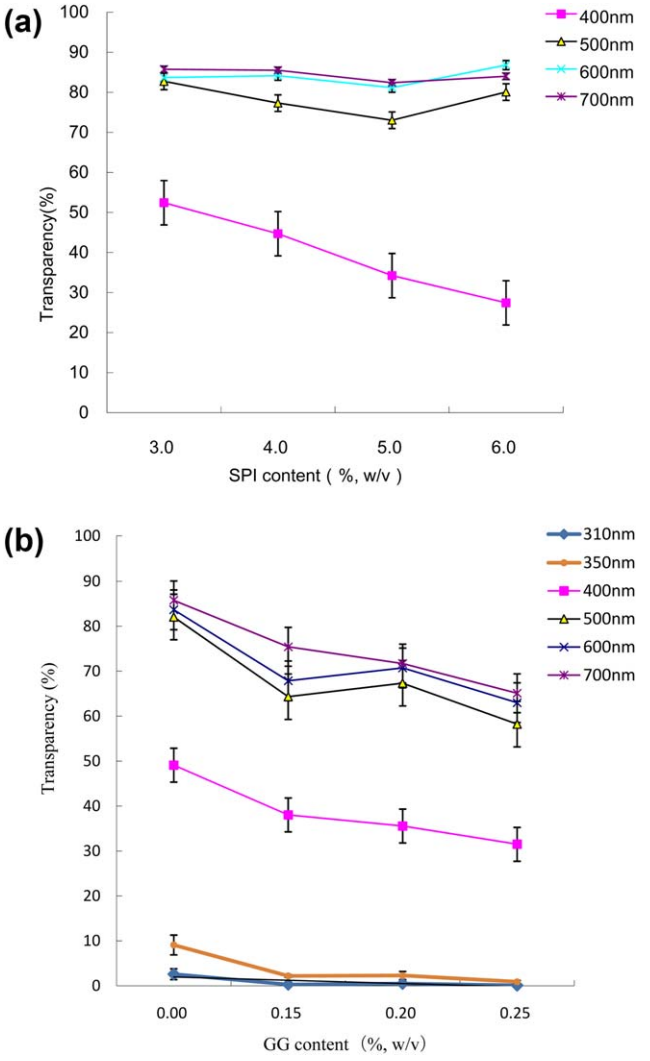

Figure 1. (a) Variation of transparency of control films IG3-0, IG4-0, IG5-0, and IG6-0 with changing SPI concentrations. (b) Variation of transparency of films IG3-0, IG3-3, IG3-4, and IG3-5 with changing GG concentrations. [Color figure can be viewed in the online issue, which is available at wileyonlinelibrary.com.]

Mechanical Properties

Improving mechanical strength of the film is desirable in order to preserve food integrality so that it can be easily processed.[28] The mechanical properties of edible films are mainly

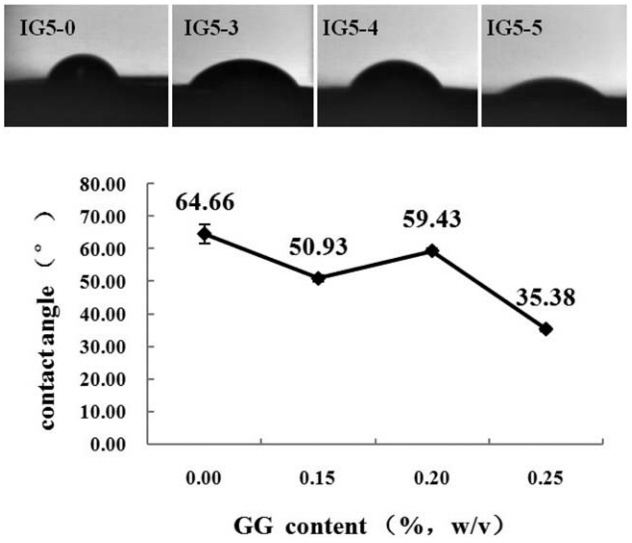

Figure 2. Contact angles values and water drop dispersion conditions of composite films IG5-0, IG5-3, IG5-4, and IG5-5.

determined through TS, TM, and BE and are strongly linked to intermolecular and intramolecular polymer interactions.[16] Table III shows the evolution of the mechanical properties for SPI films upon addition of increasing amounts of GG. Compared with SPI/GG composite films, the control SPI films exhibited poor mechanical properties besides of IG6 series. The TS and TM for SPI/GG composite films slightly increased while the BE decreased with GG addition. On the other hand, the TS and TM for SPI/GG composite films obviously increased while the BE dramatically decreased with the increase of SPI matrix concentrations. Compared to the previously reported values of SPI films, the SPI/GG composite films were almost three or four times higher TS yet lower BE than those of SPI films reported by Brandenburg.[34]

Comparison of the four series of composite films and the control films highlights that GG improves TS and TM of films. The maximum TS of the composite films was 14.92 MPa, with 5% (w/v) SPI and 0.25% (w/v) GG. The forming of SPI film relies on intermolecular disulfide bonds as well as hydrophobic, electrostatic or hydrogen bond forces.[25] By increasing the protein concentration, the amount of molecules in a unit volume is increased. After heating protein denaturation, active groups such as hydroxyl and sulfydryl are exposed and closely crosslinked during film formation, resulting in increased film compactness, and consequently, a desirable rigid structure.[35] As such, the TS and TM of the SPI/GG composite films increased with increasing SPI concentrations except IG6. However, BE values decreased with increasing SPI concentrations, likely due to decreased interchain activity.[36]

The TS of the composite films increased as GG concentration increased from 0.15 to 0.25% (w/v). This can be attributed to the ordering of the molecular structure being damaged and more hydroxyls of GG being exposed as more GG dissolved, which would benefit the formation of hydrogen bonds between SPI and GG, and film compactness. This is in accordance with experiments on GG/chitosan composite films.[21] Interestingly, the TS of the SPI/GG composite films were reduced when the SPI concentration was increased from 5 to 6% (w/v). This might be due to hydrogen bond and hydrophobic interactions between GG and SPI, resulting in SPI molecule polymerization or molecular chain winding, which is adverse to the formation of an ordered, compact network structure during the film-forming process. As GG was added, it formed complexes with SPI, which resulted that protein molecules were no more independent. Thus, the flowability turned weak, causing reduced BE of composite films compared to the control films (which was validated in SEM analyses).

Permeability

Permeability of edible protein films plays a key role in food fresh-keeping and storage stability. It refers to the ability of a film to enable small molecules (H_2O, CO_2, O_2) to permeate it. Water migration in food will not only affect its sensory quality, causing microbe reproduction, it also induces chemical enzyme reactions, which may lead to food spoilage. CO_2 and O_2 migration also extensively influence food quality and storage stability. Thus, it is essential for edible protein films to have a good degree of impermeability to H_2O, CO_2, and O_2.[21,37]

With the high-solution viscosity of SPI/GG blends at 6% (w/v) SPI, the resultant inhomogeneity produces nonuniform films. The film becomes crisp at high SPI concentrations, which is adverse when sealing at the bottleneck. Therefore, H_2O, O_2, and CO_2 permeability (WVP, OP, and COP) of three series (i.e., IG3, IG4, and IG5), totaling 12 films, are listed in Table IV.

As shown in Table IV, at constant GG concentration, the WVP of both SPI films and SPI/GG composite films increased with rising SPI concentration. In contrast, at constant SPI concentration, the WVP of composite films at varying GG concentrations first increased, and then decreased when GG concentration exceeded 0.2% (w/v). OP and COP variations showed a different tendency, and they both decreased with increasing concentrations of film substrates. The change of film permeability is in part due to the increasing intermolecular interactions of film substrates and the decreasing size of network spaces.[26,38] Moreover, film permeability is also affected by the polymer substrates' molecular structure and morphological character.[35] If the network spaces are small, or, in other words, the free space is limited, the permeation of H_2O, CO_2, and O_2 should be hindered.[37] The variation of OP and COP in the composite films was indicative of interactions between SPI and GG. Compared to the control films, the composite films' network structure can be considered more compact, as Gennadios reported for protein-based films,[25] was and is consistent with previous work on GG composite films.[18] However, the variation of WVP did not follow this trend. The presence of polyhydroxy structures in SPI and GG molecules promotes partial hydrophilic interactions between H_2O and film polymer substrates, allowing permeation of the network structure.[21] The influence of chemical reactions on water permeability was stronger than that of the network space of film, reflected in an increase in WVP, followed by a decrease with increasing GG concentrations, as shown in Table IV. This is in agreement with the conclusions drawn from film wettability and SEM experiments, where both the compatibility of SPI and GG, and interact manner changed while GG

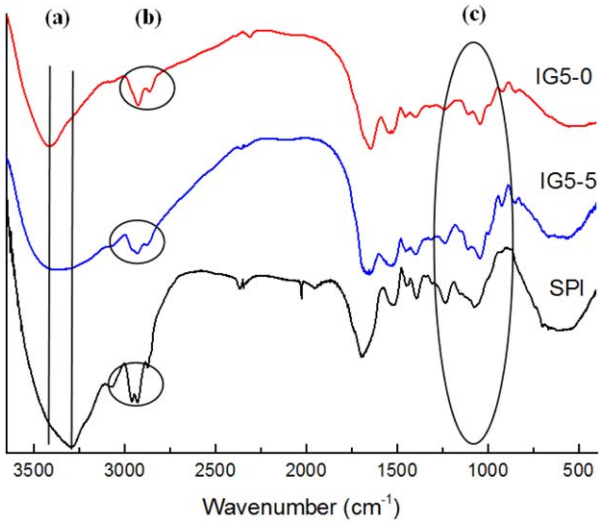

Figure 3. FTIR spectra of SPI raw material, IG5-0 film, and IG5-5 composite film. [Color figure can be viewed in the online issue, which is available at wileyonlinelibrary.com.]

concentration was above or under 0.2% (w/v). These results indicated that SPI/GG composite films had extremely low permeability. The oxygen permeability values of SPI/GG composite films were close to those of common commercial petroleum-based films.[39] The WVP values of the SPI/GG composite films were 1 orders of magnitude lower than those of SPI films and 1 orders of magnitude higher than those of PLA films.[40]

Structure and Morphology Characteristics

In order to gain insight into the films structure and interactions between SPI and GG, FTIR analysis was performed for SPI raw material, IG5-0 film, and IG5-5 composite film (Figure 3). Table V lists the positions of primary characteristic absorption peaks so as to compare the absorption peaks of control films and composite films. This was used as confirmation of SPI structural changes before and after processing as well as to highlight interactions between SPI and GG. The infrared absorption curve of SPI raw material contains N-H and O-H stretching vibration absorption peaks occurring at 3286 cm^{-1}, while C-H stretching vibrations of CH_3 and CH_2 groups occurred at 2958 and 2929 cm^{-1}. At 1647 cm^{-1}, absorption peaks of H-N-H bending mode and C=O stretching vibrations in amide I' bands were observed, whereas at 1542 and 1236 cm^{-1}, absorption peaks of N-H bending mode in amide II' bands and C-N stretching vibrations in amides III' band were observed.[17,41] Moreover, the C-O stretching vibrations' absorption peak in R-O-R, and the C-C vibrations' absorption peak or the C-O-O glycosidic bond vibrations' absorption peak of the protein molecules' ring structure occurred at 1150 and 1124 cm^{-1}. Compared to SPI raw material, the infra-red spectrum characteristic absorption peaks of IG5-0 and IG5-5 showed differences at three positions [as shown in Figure 3(a–c)]. Particularly, the absorption peak of IG5-0 at 3413 cm^{-1} showed an obvious blue shift and became wider compared with the absorption peak of SPI at 3286 cm^{-1} [Figure 3(a)], indicating that SPI was combined with glycerol, ethanol or water acquired during the film forming process. In contrast, the absorption peak of IG5-5 at 3375 cm^{-1} showed a red shift compared with that of IG5-0 film [Figure 3(a)], indicating that SPI interacted with GG by hydrogen bond interactions. The peaks characteristic at 2900–2850 $cm^{-1}$of both IG5-0 and IG5-5 moved towards lower wave numbers compared to that of SPI [Figure 3(b)]. This is likely due to changes in the molecular structure of SPI as a result of denaturation by heating. The third variation occurred at 1100 cm^{-1} [Figure 3(c)], attributable to SPI dissociation, which changed the skeleton C-C of the ring structure and glycosidic bond C-O, with a lower peak position for both IG5-0 and IG5-5.

In order to investigate the appearance differences between films and the compatibility of the blending materials, as well as to further determine the influences of SPI and GG on film properties, SEM analysis was performed to observe the surface and cross-sectional morphology of IG5-0, IG5-3, IG5-4, and IG5-5 [Figure 4(A,B)]. A clear observation was that pure SPI has favorable film forming capacity, with the ability to form a compact homogeneous microstructure [Figure 4(A), IG5-0]. The regular smooth section [Figure 4(B), IG5-0] is indicative of the fragility of pure SPI films. After adding GG, the phase morphology of the blended system significantly changed. At 0.15% (w/v) GG concentration (corresponding to IG5-3), SPI and GG did not form a homogeneous system. However, the sectional wire drawing suggested interactions between SPI and GG [Figure 4(B)], which was in accordance with the increased TS of composite films as mentioned above. As GG concentration increased from 0.15 to 0.20% (w/v) (corresponding to IG5-4), the combination of SPI and GG was enhanced, resulting in stronger compatibility [Figure 4(A)]. This was consistent with contact angle

Table V. FTIR Spectral Characteristic Absorption Peaks of SPI, IG5-0, and IG5-5 Samples

Sample	Wave number of characteristic absorption peaks (cm^{-1})							
SPI	3286	2958 2929	1685 1671 1654 1647 1639	1558 1542 1521 1508	1450 1452 1448	1236	1150 1124	1076
IG5-0	3413	2929 2875	1682 1645	1537 1524		1234	1110	1043
IG5-5	3375	2929 2877	1652	1535		1236	1108	1045

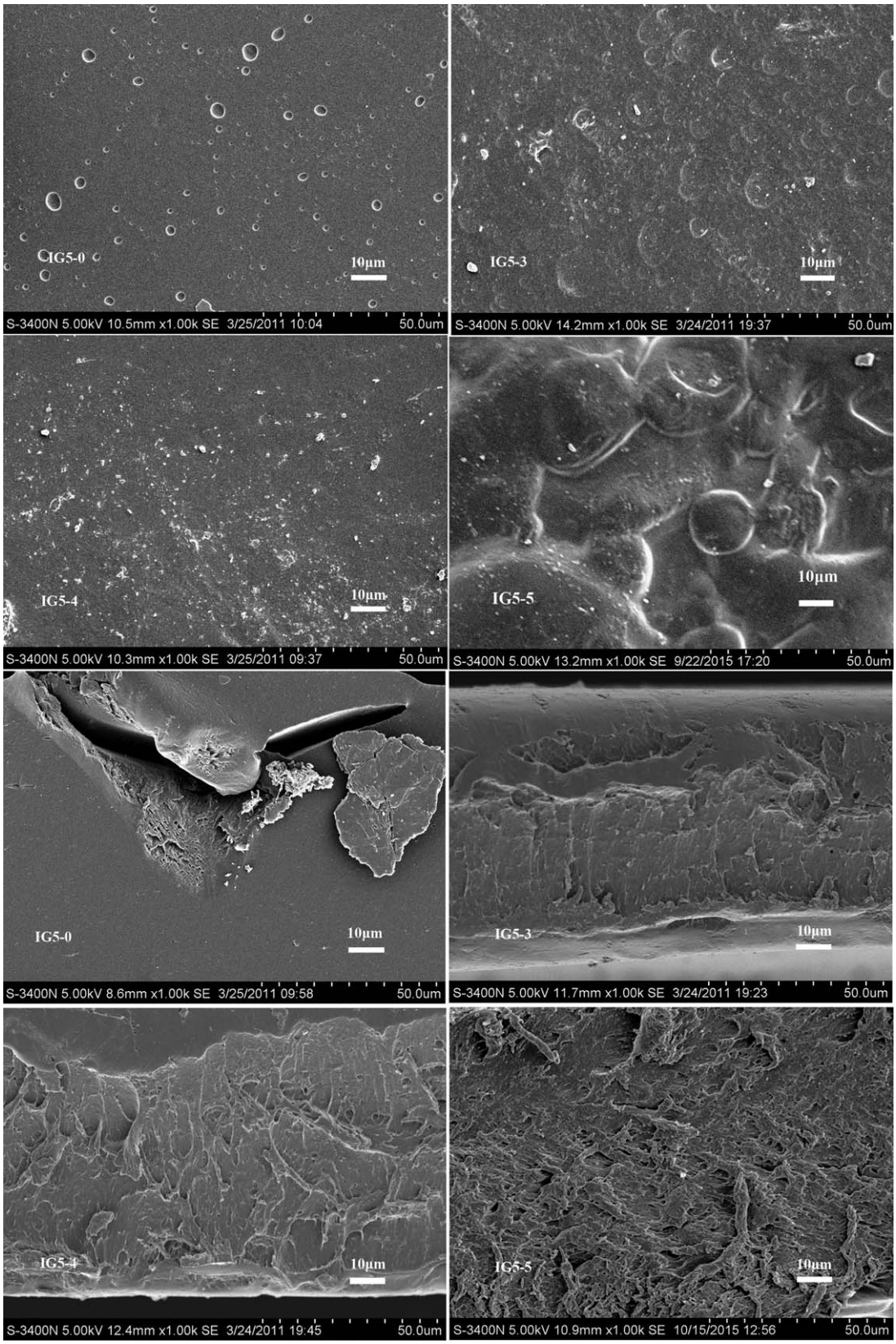

Figure 4. SEM of IG5-0, IG5-3, IG5-4, and IG5-5 films. A are surface SEMs of IG5-0, IG5-3, IG5-4, and IG5-5 films; B are cross-sectional SEMs of IG5-0, IG5-3, IG5-4, and IG5-5 films.

measurement results where the contact angle is maximal at 0.20% (w/v) GG concentration, indicating that SPI and GG formed complexes through hydrogen bonds, thereby exposing more hydrophobic groups. However, as GG concentration increased to 0.25% (w/v) (corresponding to IG5-5), surface uniformity of the IG5-5 film became bad on account of the solution viscosity increasing.

CONCLUSIONS

The SPI/GG composite films with various mass ratios between SPI and GG were successfully prepared in a method of solution casting. SPI showed good compatibility with GG due to the intermolecular interactions between these two components. With the increase of GG content, the water resistance, TS, O_2, and CO_2 barrier properties of the composite films were improved, while the elongation at break decreased. In addition, the presence of GG also improved film barrier to the light. This study suggests that SPI/GG composite films can be obtained by adding GG into the SPI matrix. The produced SPI/GG composite films have potential in packaging applications.

ACKNOWLEDGMENTS

This work was supported by the following grant: China Postdoctoral Science Foundation (No. 2013M531010); Postdoctoral Science Foundation of Heilongjiang Province (No. LBH-Z12046). The authors also gratefully acknowledge the financial support from Harbin Special Funds of Innovative Talents on Science and Technology Research Project (No. 2014RFQXJ176). We also thank Wang (Central Laboratory of Life, Northeast Agricultural University) for his help with SEM analysis.

REFERENCES

1. Siracusa, V.; Rocculi, P.; Romani, S.; Rosab, M. D. *Trends Food Sci. Technol.* **2008**, *19*, 613.
2. Zhang, H.; Wang, S.; Zheng, X.; Jiang, L.; Lv, X.; Shi, Y.; Li, L. *Eur. Food Res. Technol.* **2014**, *238*, 1049.
3. Dutta, P. K.; Tripathi, S.; Mehrotra, G. K.; Dutta, J. *Food Chem.* **2009**, *114*, 1173.
4. Wu, R. L.; Wang, X. L.; Wang, Y. Z.; Bian, X. C.; Li, F. *Ind. Eng. Chem. Res.* **2009**, *48*, 7132.
5. Cho, S. Y.; Lee, S. Y.; Rhee, C. *LWT Food Sci. Technol.* **2010**, *43*, 1234.
6. Xie, D. Y.; Song, F.; Zhang, M.; Wang, X. L.; Wang, Y. Z. *Ind. Crops Products* **2014**, *54*, 102.
7. Jensen, A.; Lim, L. T.; Barbut, S.; Marcone, M. *LWT Food Sci. Technol.* **2015**, *60*, 162.
8. Han, J.; Shin, S. H.; Park, K. M.; Kim, K. *Food Sci. Biotechnol.* **2015**, *24*, 939.
9. Tian, H.; Wang, Y.; Zhang, L.; Quan, C.; Zhang, X. *Ind. Crops Products* **2010**, *32*, 13.
10. Maria Monedero, F.; Jose Fabra, M.; Talens, P.; Chiralt, A. *J. Food Eng.* **2010**, *97*, 228.
11. Park, S.; Hettiarachchy, N.; Were, L. *J. Agri. Food Chem.* **2000**, *48*, 3027.
12. Li, Y. D.; Zeng, J. B.; Wang, X. L.; Yang, K. K.; Wang, Y. Z. *Biomacromolecules* **2008**, *9*, 3157.
13. Pan, H.; Jiang, B.; Chen, J.; Jin, Z. *Food Chem.* **2014**, *151*, 1.
14. Netravali, A. N.; Huang, X.; Mizuta, K. *Adv. Compos. Mater.* **2007**, *16*, 269.
15. Kumar, R.; Choudhary, V.; Mishra, S.; Varma, I.; Mattiason, B. *Ind. Crops Products* **2002**, *16*, 155.
16. Guerrero, P.; Stefani, P. M.; Ruseckaite, R. A.; de la Caba, K. *J. Food Eng.* **2011**, *105*, 65.
17. Guerrero, P.; Retegi, A.; Gabilondo, N.; de la Caba, K. *J. Food Eng.* **2010**, *100*, 145.
18. Dea, I. C.; Morrison, A. *Adv. Carbohydr. Chem. Biochem.* **1975**, *31*, 241.
19. Garti, N.; Madar, Z.; Aserin, A.; Sternheim, B. *LWT Food Sci. Technol.* **1997**, *30*, 305.
20. Cui, S. W.; Eskin, M. A. N.; Wu, Y.; Ding, S. *Adv. Colloid Interface Sci.* **2006**, *128*, 249.
21. Rao, M. S.; Kanatt, S. R.; Chawla, S. P.; Sharma, A. *Carbohydr. Polym.* **2010**, *82*, 1243.
22. Srivastava, M.; Kapoor, V. P. *Chem. Biodivers.* **2005**, *2*, 295.
23. Song, F.; Tang, D. L.; Wang, X. L.; Wang, Y. Z. *Biomacromolecules* **2011**, *12*, 3369.
24. Insaward, A.; Duangmal, K.; Mahawanich, T. *J. Agri. Food Chem.* **2014**,
25. Gennadios, A.; Brandenburg, A. H.; Weller, C. L.; Testin, R. F. *J. Agri. Food Chem.* **1993**, *41*, 1835.
26. Condés, M. C.; Añón, M. C.; Mauri, A. N.; Dufresne, A. *Food Hydrocolloid* **2015**, *47*, 146.
27. Tong, X.; Luo, X.; Li, Y. *Ind. Crops Products* **2015**, *67*, 11.
28. Park, S. K.; Rhee, C. O.; Bae, D. H.; Hettiarachchy, N. S. *J. Agri. Food Chem.* **2001**, *49*, 2308.
29. Tang, C. H.; Jiang, Y.; Wen, Q. B.; Yang, X. Q. *J. Biotechnol.* **2005**, *120*, 296.
30. Jangchud, A.; Chinnan, M. S. *LWT Food Sci. Technol.* **1999**, *32*, 89.
31. Kampeerapappun, P.; Aht-ong, D.; Pentrakoon, D.; Srikulkit, K. *Carbohydr. Polym.* **2007**, *67*, 155.
32. Li, H.; Liu, B. L.; Gao, L. Z.; Chen, H. L. *Food Chem.* **2004**, *84*, 65.
33. Extrand, C.; Kumagai, Y. J. *Colloid Interface Sci.* **1997**, *191*, 378.
34. Brandenburg, A.; Weller, C.; Testin, R. *J. Food Sci.* **1993**, *58*, 1086.
35. Bai, H.; Xu, J.; Liao, P.; Liu, X. J. *Plast. Film Sheeting* **2013**, *29*, 174.
36. Roy, S.; Weller, C.; Gennadios, A.; Zeece, M.; Testin, R. *J. Food Sci.* **1999**, *64*, 57.
37. Miller, K.; Krochta, J. *Trends Food Sci. Technol.* **1997**, *8*, 228.
38. Di Pierro, P.; Mariniello, L.; Giosafatto, C. V. L.; Masi, P.; Porta, R. *Food Biotechnol.* **2005**, *19*, 37.
39. Gennadios, A.; WELLER, C.; Testin, R. *J. Food Sci.* **1993**, *58*, 212.
40. Rhim, J. W.; Mohanty, A. K.; Singh, S. P.; Ng, P. K. *J. Appl. Polym. Sci.* **2006**, *101*, 3736.
41. Liu, D.; Zhang, L. *Macromol. Mater. Eng.* **2006**, *291*, 820.